BIOCHEMISTRY
including biophysical chemistry & molecular biology

Current Topic

pubs.acs.org/biochemistry

Structure and Mechanism of DNA Polymerase β

William A. Beard and Samuel H. Wilson*

Laboratory of Structural Biology, National Institute of Environmental Health Sciences, National Institutes of Health, 111 T. W. Alexander Drive, P.O. Box 12233, MD F3-01, Research Triangle Park, North Carolina 27709, United States

ABSTRACT: DNA polymerase (pol) β is a small eukaryotic DNA polymerase composed of two domains. Each domain contributes an enzymatic activity (DNA synthesis and deoxyribose phosphate lyase) during the repair of simple base lesions. These domains are termed the polymerase and lyase domains, respectively. Pol β has been an excellent model enzyme for studying the nucleotidyl transferase reaction and substrate discrimination at a molecular level. In this review, recent crystallographic studies of pol β in various liganded and conformational states during the insertion of right and wrong nucleotides as well as during the bypass of damaged DNA (apurinic sites and 8-oxoguanine) are described. Structures of these catalytic intermediates provide unexpected insights into mechanisms by which DNA polymerases enhance genome stability. These structures also provide an improved framework that permits computational studies to facilitate the interpretation of detailed kinetic analyses of this model enzyme.

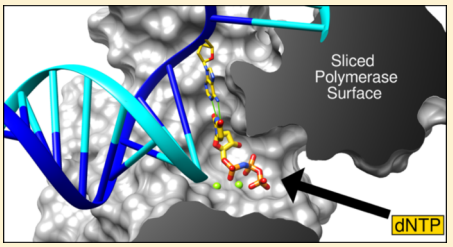

DNA polymerases catalyze template-dependent DNA synthesis during genome replication and repair. These enzymes are responsible for preferentially binding and incorporating a nucleotide, from a pool of chemically and structurally similar molecules, that correctly base pairs with the appropriate templating base. DNA polymerase (pol) β has served as a model enzyme for studying this fundamental task, providing a detailed understanding of the events during substrate selection. Pol β is the smallest cellular DNA polymerase (335 residues, 39 kDa) and lacks a 3′ → 5′ proofreading exonuclease activity that enhances the accuracies of replicative DNA polymerases (e.g., pol ε and pol δ). On the basis of its primary sequence, pol β belongs to the X-family of DNA polymerases.[1] This review will highlight recent advances and insights provided by the structural characterization of pol β in various liganded and conformational states. For earlier kinetic and structural descriptions, see previous in-depth reviews.[2,3]

BIOLOGICAL ROLE

Endogenous and environmental agents continually modify genomic DNA, resulting in physical damage or modification that results in steady-state levels of 50000—200000 apurinic/apyrimidinic (AP) sites per eukaryotic cell.[4] AP sites are generated through spontaneous depurination or lesion specific enzymatic hydrolysis of the *N*-glycosyl bond between the deoxyribose and base. The rate of spontaneous depurination has been estimated to be ~10^4 depurinations per cell per day.[5] The base excision repair (BER) pathway (Figure 1) is responsible for removing simple base lesions and AP sites in DNA. Pol β contributes two enzymatic activities, DNA synthesis and deoxyribose phosphate (dRP) lyase, during the repair of AP sites.

AP sites represent potentially dangerous lesions because they can be mutagenic and cytotoxic. AP endonuclease 1 incises the AP site, resulting in 3′-hydroxyl and 5′-dRP termini. The dRP group is excised by the lyase activity of pol β, resulting in a 5′-phosphate and a one-nucleotide gap (i.e., a single templating base). Pol β fills this single-nucleotide gap, resulting in nicked DNA that will subsequently be ligated to restore DNA's native structure.

As discussed in detail below and elsewhere,[6,7] pol β and other members of the X-family of DNA polymerases have evolved to fill short DNA gaps during essential cellular transactions. In a mouse model system, the loss of pol β results in embryonic lethality; however, cultured embryonic mouse fibroblasts are viable.[8] These cells are hypersensitive to genomic toxicants because of the accumulation of cytotoxic repair intermediates.[9] In addition to its enzymatic activities, pol β physically interacts with other key BER factors that hasten repair at AP sites.[10]

The fundamental role that pol β plays in BER and high-fidelity gap-filling DNA synthesis implicates pol β and BER as tumor suppressors.[11,12] Consistent with this idea is the observation that a high percentage of tumors have variants of pol β. These often have altered fidelity or catalytic activities and can induce cellular transformation.[13] Many of these variants have amino acid changes that are distant from the polymerase or lyase active sites. It remains to be seen whether these alterations affect critical protein−protein interactions necessary for efficient BER or critical protein dynamic behavior that influences catalytic activity and/or fidelity (see below).

MINIMAL REACTION PATH FOR NUCLEOTIDE INSERTION

DNA polymerases are believed to follow the general pathway outlined in Scheme 1. The detailed kinetic and equilibrium constants are sensitive to the identity of the polymerase and

Received: January 31, 2014
Revised: March 26, 2014
Published: April 10, 2014

dx.doi.org/10.1021/bi500139h | *Biochemistry* 2014, 53, 2768−2780

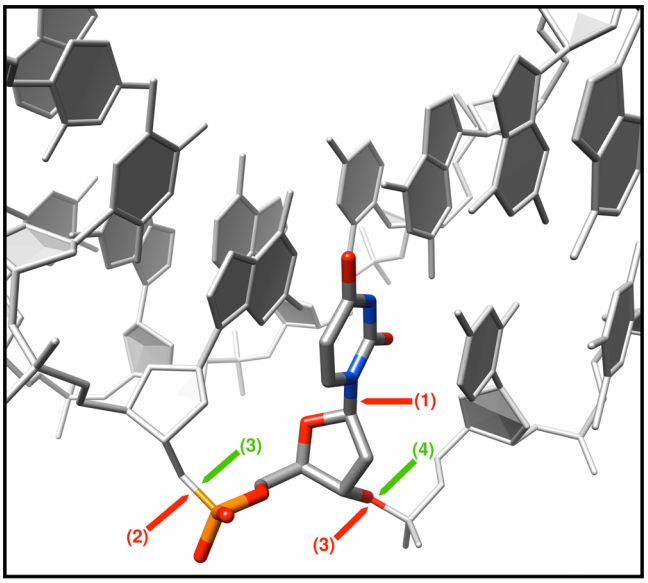

Figure 1. Base excision repair. Base excision repair involves the removal of a damaged nucleotide (red pointers) from DNA. It is replaced with an undamaged nucleotide (green pointers). The damaged base is removed by a damage specific DNA glycosylase (1) that hydrolyzes the N-glycosidic bond between the deoxyribose and damaged base. In this image, uracil would be removed by uracil DNA glycosylase. AP endonuclease 1 incises the sugar–phosphate backbone 5′ to the AP site (2). The lyase domain of pol β (3) removes the 5′-dRP group (red pointer), and the polymerase domain inserts a nucleotide in a template-dependent reaction (green pointer). DNA ligase (4) seals the nicked DNA, resulting in restoration of the original DNA structure.

substrates (e.g., base and sugar of the nucleoside triphosphate and DNA sequence context). In addition, the nature (kinetic and thermodynamic) of the conformational changes(s) before and after chemistry has been the subject of a long-standing debate as well as their impact on substrate discrimination (i.e., fidelity).[14] Steady-state kinetic analyses indicate that pol β follows an ordered binding of substrates;[15] after binding DNA (Scheme 1, step 1), DNA polymerases preferentially bind a nucleoside triphosphate (dNTP) that preserves Watson–Crick hydrogen bonding as dictated by the template (coding) base (step 2). The ternary substrate complex undergoes a global conformational change (step 3). While many DNA polymerases undergo a large subdomain motion, more subtle conformational adjustments that either hasten or deter the subsequent chemical step (step 4) occur. Following chemistry, the ternary product complex undergoes a conformational change (step 5) that facilitates PP_i release (step 6). At this point, the extended product (DNA_{+1}) is released (single-nucleotide insertion) or serves as substrate DNA for another round of nucleotide insertion following translocation (processive DNA synthesis). DNA synthesis also requires at least two divalent metal ions. These are not explicitly shown in Scheme 1 but are discussed in detail below.

STRUCTURAL INTERMEDIATES

Structural biology offers a unique opportunity to visualize well-populated intermediate states during catalytic cycling at a molecular level. This approach requires that intermediate states be trapped using modified enzymes, inert cofactors, or substrate analogues. Alternatively, reactions can be initiated in the crystal and stopped at defined moments by rapid freezing. In each case, the structures should be interpreted in the context of a kinetic–thermodynamic model for ligand binding and catalysis. This is especially challenging because structural models often represent static snapshots of dynamic events. Computational studies that bridge the observed intermediate states can be very useful in correlating structural and kinetic observations.[16] Crystallographic structures of most of the intermediates depicted in Scheme 1 have been determined at high resolution and provide molecular insights by which an induced-fit model bestows substrate specificity (Table 1). We next describe salient features of available crystallographic structures of the intermediates outlined in Scheme 1.

Apoenzyme (I). Controlled proteolytic or chemical cleavage of pol β first demonstrated that it is folded into discrete domains.[17] The structure of the unliganded apoenzyme was first reported in 1994.[18] It confirmed that the enzyme was folded into two domains: an amino-terminal 8 kDa domain and the 31 kDa polymerase domain (Figure 2). Consistent with sedimentation velocity measurements[19] and small-angle X-ray scattering studies of the apoenzyme,[20] the global structure displays an extended conformation (Figure 2A). It is now recognized that the dRP lyase activity resides in the amino-terminal domain.[21,22] Like other DNA polymerases, the

Scheme 1. Minimal DNA Polymerase Reaction Pathway[a]

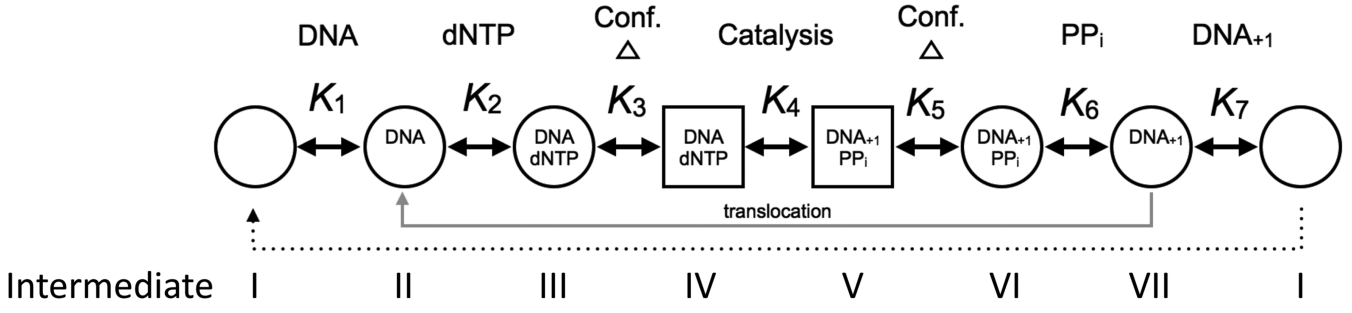

[a]After binding DNA (step 1), the nucleotide triphosphate binds, forming an initial ternary complex (circle, step 2). The polymerase–substrate complex undergoes rapid conformational adjustments that lead to a productive ternary substrate complex (square, step 3). Catalysis (step 4) leads to a postchemistry product ternary complex. Product release occurs concurrent with or following conformational changes (step 5) that facilitate PP_i release (step 6). Translocation of the nascent base pair upstream vacating the active site prepares the polymerase for the next insertion event (gray solid line). Alternatively, product DNA_{+1} may dissociate from the polymerase (step 7), terminating DNA synthesis. While two divalent metals (Mg^{2+}) are required for catalysis, they are not explicitly shown in this scheme. See the text for the role of these metals.

dx.doi.org/10.1021/bi500139h | *Biochemistry* 2014, 53, 2768–2780

Table 1. Crystallographic Structures of Pol β Catalytic Intermediates

intermediate (conformation)[a]	ligand	PDB entry	refs
I (O)	none	1BPD, 3UXN	18, 78
II (O)	DNA	1BPX, 3ISB	30, 66
III (O)	DNA, dNTP	4F5N, 4F5O, 4F5P[b]	34
IV (C)	DNA, dNTP	2BPF, 1BPY, 2FMS, 1HUO, 4KLD, 4KLE, 4KLF, 3C2L,[b] 3C2M,[b] 4KLP, 4KLQ,[b] 4KLS[b]	30, 36, 37, 39, 46, 65
V (C)	DNA_{+1}, PP_i	1HUZ, 4KLG, 4KLH, 4KLI, 4KLJ, 4KLL, 4KLM, 4KLO, 4KLT[b]	39, 46
VI (O)	DNA_{+1}, PP_i	–	–
VII (O)	DNA_{+1}	1BPZ, 1TV9,[b] 1TVA,[b] 4KLU[b]	30, 39, 79

[a]The global conformation is specified as open (O) or closed (C). [b]Refers to a structure with an active site mismatch.

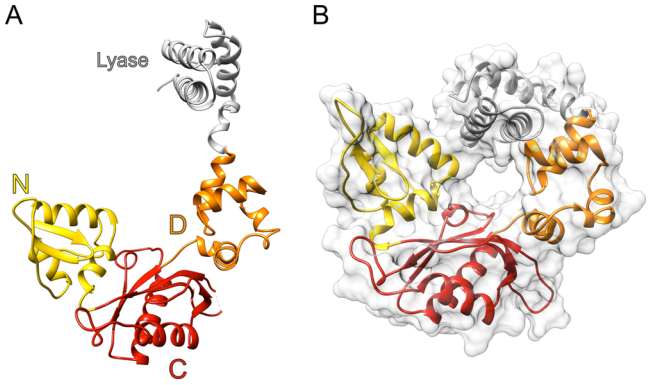

Figure 2. Domain and subdomain organization of DNA polymerase β. Ribbon representation of pol β illustrating the polymerase (colored) and amino-terminal lyase (gray) domains. The polymerase domain is composed of three subdomains: D, orange; C, red; and N, yellow. These correspond to the thumb, palm, and fingers subdomains, respectively, of DNA polymerases that utilize an architectural analogy to a right hand. (A) The structure of the apoenzyme indicates that it forms an extended structure (PDB entry 1BPD).[18] (B) The molecular surface (semitransparent) of pol β bound to single-nucleotide gapped DNA (PDB entry 3ISB)[66] exhibits a global doughnutlike structure in which the lyase domain interacts with the N-subdomain of the polymerase domain.

polymerase domain has a modular organization with three functionally distinct subdomains. The catalytic subdomain coordinates two divalent metal cations (Mg^{2+}) that facilitate DNA synthesis. The other two subdomains are spatially situated on opposite sides of the catalytic subdomain. While the catalytic subdomains of X- and C-family DNA polymerases share structural homology, those from other families (e.g., members of the A- and B-families) exhibit a similar but unique fold.[23] Structures of A-, B-, and Y-family polymerases have likened these enzymes to a right hand with fingers, palm, and thumb subdomains.[24−26] However, this nomenclature is the opposite of that originally proposed for pol β.[18] Thus, there is not a consistent usage of the handlike nomenclature in the literature. Because the handlike architectural analogy lacks functional insight, we use functionally based designations for the subdomains. The polymerase domain includes the C-subdomain (catalytic), the D-subdomain (DNA binding), and the N-subdomain (nascent base pair binding) that are equivalent to the palm, thumb, and fingers subdomains, respectively, of right-handed DNA polymerases (Figure 2).[27]

Binary DNA Substrate Complex (II). In contrast to replicative DNA polymerases that are targeted to the growing 3′-primer terminus at the double-stranded−single-stranded DNA junction, pol β is targeted to the 5′-margin in gapped DNA. In contrast to the extended protein conformation of the apoenzyme, the binding to single-nucleotide gapped DNA results in a doughnutlike protein conformation (Figure 2B). The lyase domain strongly binds the 5′-phosphate or 5′-dRP BER intermediate in gapped DNA.[28] The product of the dRP lyase reaction generates a 5′-phosphate; transient-state kinetic characterization of the dRP lyase reaction indicates that it is significantly more rapid than single-nucleotide insertion, so that DNA synthesis would occur using a "clean" gap (i.e., the 3′- and 5′-margins in the gap are appropriate for their respective enzymatic activities; DNA synthesis and subsequent ligation).[29]

In the binary one-nucleotide gapped DNA structure, the 5′-phosphate in the gap is hydrogen bonded to Lys35 and Lys68 (Figure 3A).[30] Importantly, pol β binds tightly to the 5′-phosphate only when there is single-stranded DNA adjacent to the 5′-phosphate. This can be nongapped single-stranded DNA because a 3′-primer terminus is not required for optimal binding.[28] Accordingly, pol β is expected to bind to the 5′-phosphate in a DNA gap of any size. The observation that it will processively (i.e., insert several nucleotides before dissociating from the DNA substrate) fill short gaps (fewer than six nucleotides) suggests that the lyase domain tethers the polymerase domain to the downstream position in gapped DNA. When the primer terminus (i.e., 3′-OH) is within six nucleotides of the 5′-phosphate on the downstream DNA strand, the proximity of the polymerase domain to the primer terminus would hasten processive DNA synthesis.

The α-helical 8 kDa lyase domain includes a structural motif that binds a monovalent metal interacting with the DNA backbone downstream of the single-nucleotide gap (Figure 3B).[31] This helix−hairpin−helix (HhH) motif (residues 55−79) includes Lys72 that serves as the primary amine that forms a Schiff base intermediate during excision of the 5′-dRP moiety in BER.[32] In addition, the D-subdomain interacts with the DNA sugar−phosphate backbone of the duplex DNA upstream of the gap utilizing a second HhH motif (Figure 3B, residues 92−118). This HhH motif also interacts with the primer strand phosphate backbone through a monovalent metal ion. Thus, the two HhH motifs are observed to make DNA backbone interactions with each end of the incised DNA strand. In the structure of the binary gapped DNA complex, the DNA is bent ∼90° as it enters the polymerase active site. The sharp bend occurs at the 5′-phosphodiester bond of the templating base. The function of the HhH motifs appears to be a sequence nonspecific phosphate backbone binding motif that stabilizes the pronounced bend observed in the gapped DNA structure. The abrupt bend in the DNA also exposes the terminal base pairs of each DNA duplex that is situated in the gap. His34 of the lyase domain interacts with the first base pair of the downstream duplex, whereas the N-subdomain contributes interactions with the nascent base pair in the closed ternary complex (see below). The altered path of the template strand as it enters the polymerase active site is a general feature observed in most structures of substrate complexes of DNA polymerases.

Open Ternary Substrate Complex (III). Pol β and members of the A- and B-families of DNA polymerases exhibit

dx.doi.org/10.1021/bi500139h | Biochemistry 2014, 53, 2768−2780

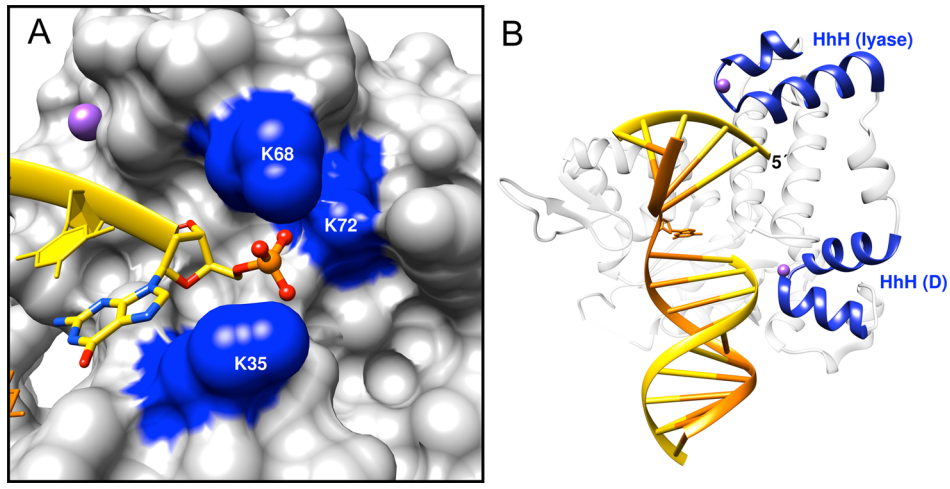

Figure 3. DNA binding. (A) Surface representation of the lyase domain highlighting the 5′-phosphate binding pocket (PDB entry 3ISB).[66] The 5′-phosphate is hydrogen bonded to Lys35 (K35) and Lys68 (K68). Lys72 serves as the nucleophile for removal of the 5′-dRP intermediate during BER. (B) The lyase domain and the D-subdomain each have a HhH motif (blue ribbons) that interacts with the DNA backbone of the incised DNA strand (yellow) downstream and upstream of the gap, respectively. This motif binds a monovalent cation (Na^+, purple) making sequence nonspecific interactions with the DNA backbone. The template strand is colored orange, and most of the nucleotides are illustrated in a ladder representation. The coding templating base in the gap is shown as sticks. The 5′-margin in the gap of the incised strand is indicated.

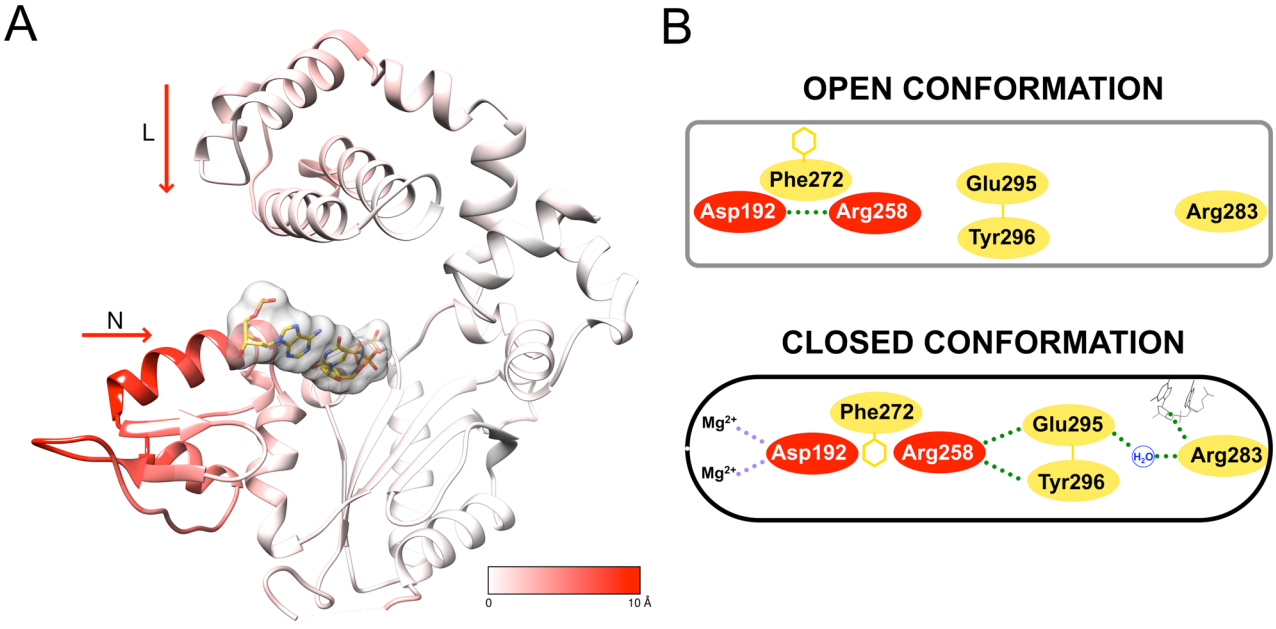

Figure 4. Nucleotide-induced conformational changes. (A) Ribbon representation of the single-nucleotide gapped DNA binary pol β complex (PDB entry 3ISB).[66] The ribbon is colored according to the protein backbone displacement upon formation of the ternary substrate complex (PDB entry 2FMS),[37] from white (0 Å) to red (10 Å). The nascent base pair is also illustrated with a semitransparent surface representation (PDB entry 2FMS). Significant domain and subdomain repositioning occurs exclusively in the lyase domain and N-subdomain. (B) In the open conformation, Arg283 (N-subdomain, yellow) does not interact with other key residues, but in the closed conformation, it interacts with the templating (coding) base, the upstream template nucleotide, and Glu295 (green dotted lines). Consequently, the position of the N-subdomain is structurally transmitted to the active site through a series of interactions involving Arg283 and Asp192 that coordinates (purple dotted lines) both active site Mg^{2+} ions. This is also accompanied by altered interactions of Glu295/Tyr296 with Arg258 in the open and closed forms. Phe272 is postulated to transiently interfere with interactions between Asp192 and Arg258, permitting an interaction with Glu295/Tyr296. Residues in the C-subdomain are colored red. Panel B was adapted from ref 40.

a rapid repositioning of the N-subdomain (fingers) upon nucleotide binding to close around the nascent base pair (Figure 4A). In the presence of an incoming dNTP, the closed complex of the wild-type enzyme is stable (i.e., $K_3 \gg 1$).[33] By weakening interactions of the N-subdomain believed to stabilize the closed complex, an intermediate complex with an incoming nucleotide bound to the open conformation was determined.[34] Substituting lysine for arginine at residue 283 (Figure 4B) of α-helix N results in a mutant polymerase with moderately reduced catalytic efficiency.[35] The structure reveals that the coding template base facilitates binding of the incoming correct dNTP to the open form of pol β through Watson−Crick hydrogen bonds (Figure 5A). However, the nascent base pair is severely buckled, because the sugar/

dx.doi.org/10.1021/bi500139h | *Biochemistry* 2014, 53, 2768−2780

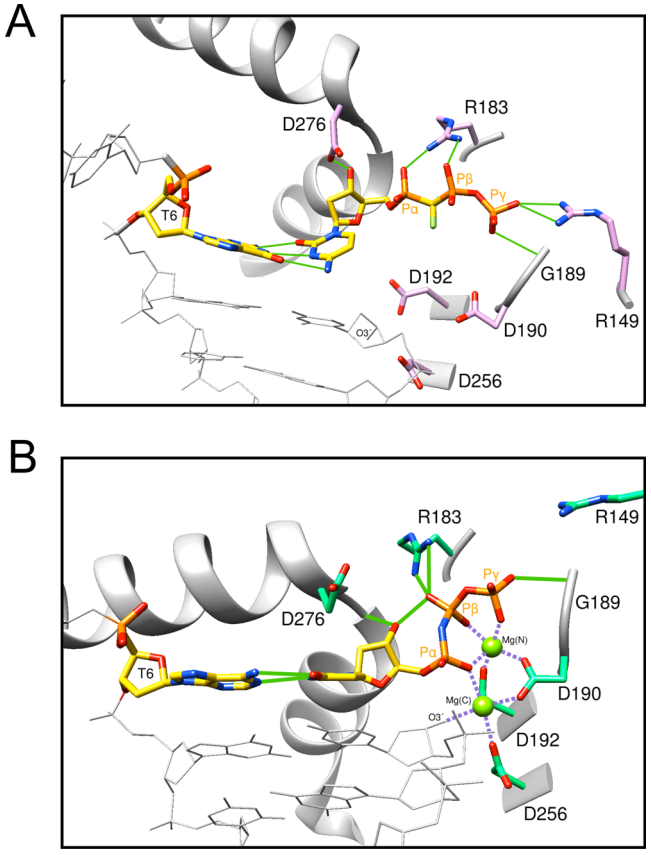

Figure 5. Nucleotide binding to pol β. (A) A ternary substrate complex with the correct incoming nucleotide was trapped in the open conformation using a mutant of pol β that destabilizes the closed conformation.[34] In this structure (PDB entry 4F5N), protein side chains coordinate the extended anionic triphosphate moiety of the incoming nonhydrolyzable dCTP analogue, dCMP(CF_2)PP. Although the nascent base pair (yellow carbon atoms) is severely buckled, the incoming cytosine base hydrogen bonds (green lines) with the templating guanine. Asp276 (D276) hydrogen bonds with O3′ of the incoming nucleotide, while Arg183 (R183) coordinates nonbridging oxygens on the α-phosphate (Pα) and β-phosphate (Pβ) of the incoming nucleotide. Arg149 (R149) and Gly189 (D189) coordinate the γ-phosphate (Pγ) of the incoming nucleotide. Active site aspartates (D190, D192, and D256) that coordinate active site metals are also indicated. The templating (coding) nucleotide and primer terminus are also indicated (T6 and O3′, respectively). (B) The active site structure and metal coordination of the precatalytic ternary substrate complex (PDB entry 2FMS) are consistent with a two-metal mechanism for nucleotidyl transfer. This closed structure was trapped with an inert dUTP analogue (dUMPNPP).[37] Importantly, the primer terminus O3′ coordinates the catalytic Mg^{2+}, labeled Mg(C). The catalytic Mg^{2+} also coordinates all three active site aspartates (purple dashed lines). In this structure, O3′ of the primer terminus is 3.4 Å from the α-phosphate of dUMPNPP. A nucleotide binding metal, Mg(N), coordinates nonbridging oxygens on all three phosphates. The protein coordination of the triphosphate also differs from that observed in the absence of metals. Arg183 now only coordinates the β-phosphate, and Arg149 has lost its direct contact with Pγ.

triphosphate moieties interact with protein side chains that have not moved to their closed positions. Surprisingly, the negative charge on the incoming nucleotide triphosphate was neutralized through protein interactions (Figure 5A). Although free nucleotides are usually associated with a magnesium ion, the nucleotide–metal complex exists in several coordination states and diastereoisomers. The ability to trap a metal-free complex suggests that the polymerase has a strong influence on metal coordination and triphosphate reorganization. It remains to be determined how the polymerase directs and/or deters (e.g., for an incorrect nucleotide) the metal coordination state of the incoming nucleotide.

Closed Ternary Substrate Complex (IV). Precatalytic closed crystallographic structures have been trapped by employing inert analogues of catalytic participants; the dideoxy-terminated primer (i.e., absence of primer O3′),[36] an incoming nucleotide where the bridging oxygen between the α- and β-phosphates has been replaced with an imido or methylene group;[37,38] or substituting calcium for magnesium.[39] All three approaches have been successfully utilized to trap closed ternary complexes of pol β. The structures show that the N-subdomain has closed around the nascent base pair (Figures 4 and 5). This global structural transition induces many subtle conformational adjustments that lead to conformational activation. One key aspect of this activation is that Asp192 is released from its salt bridge interaction with Arg258, permitting it to coordinate both the catalytic and nucleotide binding metals (Figure 4B). The importance of this conformational activation is illustrated by the observation that mutagenesis of Arg283 and Glu295, which are >10 Å from the active site, dramatically decreases activity and the extent of conformational activation.[35,40−42]

Another key conformational adjustment resides in the precise positioning of O3′ of the deoxyribose of the primer terminus. The catalytic metal coordinates a nonbridging oxygen of the α-phosphate of the incoming nucleotide as well as O3′ of the primer terminus. In the absence of this metal or O3′ (i.e., dideoxy-terminated primer), crystallographic structures indicate that the sugar pucker is 2′-endo; however, binding of the catalytic magnesium alters the sugar pucker of the primer terminus (3′-endo), thereby repositioning O3′ for in-line attack on the α-phosphate of the incoming nucleotide. These conformational adjustments facilitate binding of the catalytic magnesium necessary to activate the primer 3′-OH and position the α-phosphate of the incoming dNTP. Because the closed ternary substrate complex can be determined without the catalytic magnesium, it is believed that this is the last component that binds to complete the precatalytic complex. This is also consistent with the reported binding affinity for the catalytic metal.[43]

Recently, ternary complex crystallographic structures of intermediate complexes undergoing nucleotidyl transfer have been captured with natural substrates and metals.[39,44] This is achieved by generating crystals of precatalytic substrate ternary complexes in the presence of the inert metal Ca^{2+} and then initiating the reaction through ion exchange with Mg^{2+}. The reaction is stopped by freezing the crystal as the reaction progresses (i.e., after a defined time period), and the structure is determined. Unexpectedly, an additional divalent metal site is observed transiently bridging oxygen atoms on the products (Figure 6A). Thus, this metal is associated with the product state and postulated to be involved in pyrophosphorolysis, the reverse reaction of DNA synthesis (Scheme 1, k_{-4}).[39] The presence of this metal is expected to be unique to X- and Y-family DNA polymerases because other DNA polymerases have a conserved basic side chain that occupies this position.[39,45] Those side chains appear to have multifunctional roles that are dependent on the stage of the reaction: a role in polarizing Pα of the incoming nucleotide, stabilizing the negative charge developing on the products, and modulating K_4 (i.e., the

dx.doi.org/10.1021/bi500139h | Biochemistry 2014, 53, 2768−2780

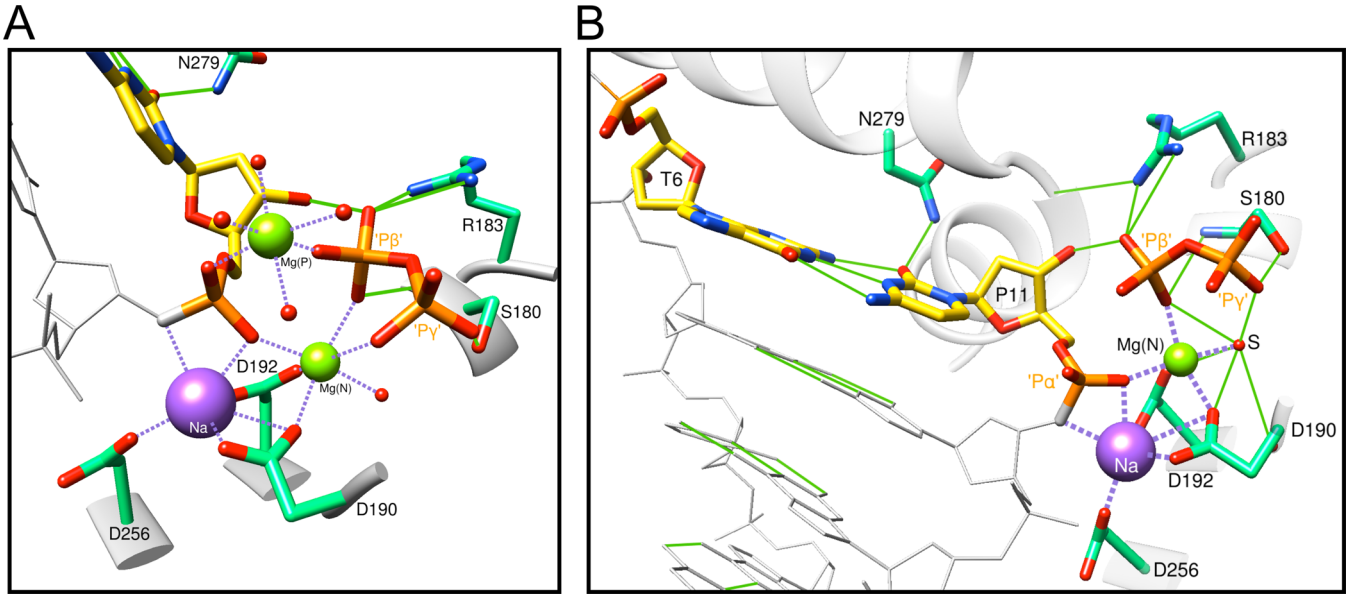

Figure 6. Structures of the closed product complex of pol β. (A) As the nucleotidyl transfer reaction proceeds in the crystal, an additional divalent metal is observed in the closed product complex.[39] After a 40 s reaction in the crystal (PDB entry 4KLG), the active site structure reveals a new metal [Mg(P)] that bridges the two products, i.e., coordinates nonbridging oxygens on the phosphates of the incorporated dCMP and the remnant β-phosphate of PP_i (yellow carbons). Water molecules (red spheres) complete the octahedral coordination (purple dashed lines). A sodium ion (purple sphere, Na^+) replaces the catalytic magnesium, but the nucleotide-associated Mg^{2+} still coordinates nonbridging oxygens on the phosphates of the products (dCMP and PP_i). (B) After an extended reaction in the crystal (45 min, PDB entry 4KLL), the polymerase remains closed, but the PP_i appears to be preparing to dissociate. In this case, a water molecule (S) replaces the remnant of the γ-phosphate for nucleotide metal coordination. Hydrogen bonds are displayed as green lines.

internal chemical equilibrium). In addition, there are basic side chains in the N-subdomain that stabilize the incoming dNTP in the closed conformation.

Closed Ternary Product Complex (V). After chemistry, the ternary product complex remains in the closed conformation. However, there are subtle active site changes concomitant with chemistry. The resulting phosphodiester bond alters the coordination state of the catalytic Mg^{2+}, hastening its dissociation and its replacement with Na^+. In contrast, the nucleotide-associated Mg^{2+} remains in the active site coordinating aspartates and PP_i (Figure 6B). After longer periods of time, the PP_i coordination is altered as one phosphate, the Pγ remnant, is stripped from the nucleotide metal by a competing water molecule, indicating that metal solvation may play a role in PP_i dissociation and/or subdomain opening. Surprisingly, the product complex after correct nucleotide insertion (i.e., nicked DNA) remains in a closed conformation with bound PP_i even with extended incubations. Because catalytic cycling in solution occurs much more rapidly, other factors such as crystal packing or excessive divalent metals are influencing the open or closed state of the enzyme. The ternary product complex can also be formed by crystallizing pol β with nicked DNA (annealed oligonucleotides) to generate an open binary complex. Addition of PP_i and Mg^{2+} produced a closed ternary product complex similar to that described above in which the nucleotide and product metals sites are occupied with Mg^{2+} and the catalytic metal site is occupied with Na^+ (Figure 6A). A reverse reaction is not observed probably because of the unfavorable equilibrium for this reaction.

Previously, a similar approach employing an exchange-inert nucleotide analogue, Cr^{3+}-2′-deoxythymidine 5′-β,γ-methylene-triphosphate, bound to pol β could turn over in the crystal after the addition Mn^{2+}.[46] As described above, the catalytic metal ion was not observed, indicating that it had dissociated after chemistry. Additionally, the polymerase remains in the closed conformation with bound products. Because Cr^{3+} does not permit ligand exchange and is bound at the nucleotide binding metal site, it remained bound to the oxygens of the product phosphates (incorporated TMP and PCP) so that solvent could not compete for metal coordination, hastening dissociation of the PP_i analogue. These structural observations are consistent with pyrophosphate exchange experiments with T7 DNA polymerase that suggest that PP_i release occurs with or after a postchemistry conformational change (Scheme 1, step 5).[47]

Binary DNA Product Complex (VII). As described above, pol β can be crystallized after being incubated with annealed oligonucleotides that create a nicked product DNA.[30,39] In this situation, pol β is in the open conformation with the primer terminus in the nascent base pair binding pocket. While addition of PP_i creates a closed ternary product complex, the structure of an open ternary product complex (Scheme 1, complex VI) has not been determined probably because of the weak affinity of PP_i and the inclination of the polymerase to close with bound products. Mutagenesis of the polymerase to destabilize the closed form might overcome this obstacle.

DNA POLYMERASE NUCLEOTIDYL TRANSFERASE

A model for the nucleotidyl transferase enzymatic mechanism is supported by structures of ternary substrate complexes.[30,37,39] The chemical mechanism proceeds by an in-line nucleophilic attack of the Mg^{2+}-activated primer O3′ anion on the α-phosphate of the incoming nucleotide, leading to a pentacoordinated bipyramidal α-phosphate transition state. The transition state is resolved by release of PP_i from the opposite side of the attacking nucleophile, resulting in stereochemical inversion about the α-phosphorus of the newly incorporated nucleotide. The pol β active site includes

dx.doi.org/10.1021/bi500139h | Biochemistry 2014, 53, 2768−2780

three conserved acidic residues that bind two divalent magnesium ions. One Mg^{2+} (nucleotide binding metal) coordinates two aspartate residues (Asp190 and Asp192) and the triphosphate moiety of the incoming nucleotide, thereby facilitating nucleotide binding. The other Mg^{2+} (catalytic) coordinates all three active site aspartates (Asp190, Asp192, and Asp256) and O3′ of the primer terminus (Figures 4A and 5B). It lowers the pK_a of the primer terminus 3′-OH, hastening attack on Pα of the incoming nucleotide, and serves as a general base upon O3′ activation.[48] Thus, the pK_a values of both the donor (primer O3′) and the acceptor group (OD2 of Asp256) are modulated by the catalytic Mg^{2+}.

Site-directed mutagenesis of Asp256 coupled with crystallographic, activity−pH profile, and computational studies confirms that this residue plays a fundamental role in nucleotidyl transfer.[49] In this study, quantum calculations revealed the transfer of charge into the catalytic metal and a decrease in the charge of Asp256(OD2) that accompanies the proton jump from the primer terminus (O3′) to OD2. In spite of the loss of the proton, the charge on O3′ remains almost constant, facilitating its approach toward Pα of the incoming nucleotide. Interestingly, in the structure of a D256E mutant, a water molecule replaces OD2 of Asp256, and this water is seen to coordinate the catalytic Mg^{2+}. However, in quantum calculations, this water does not substitute for Asp256(OD2) in the transfer of charge to the catalytic Mg^{2+}. In this situation, the water molecule jumps to OE1 of Glu256, and the energy barrier for the transition state is much higher than that for the wild-type enzyme.[49] The critical role of Asp256(OD2) appears to be facilitated by a stabilizing salt bridge interaction between Asp256(OD1) and the nearby Arg254. In the D256E mutant, Arg254 is repositioned and does not interact with Glu256.

FIDELITY

Correct Nucleotide Insertion Efficiency Controls Fidelity. DNA polymerase fidelity, specificity, and discrimination are relative kinetic terms used to describe the probability of a polymerase producing a base substitution error (i.e., mismatch). The base substitution error frequency for DNA replication and repair polymerases is generally between 10^{-3} and $>10^{-6}$.[50] These frequencies represent one error per 1000 and 1 million nucleotides synthesized, respectively. These levels of discrimination are far greater than those predicted by free energy differences between matched and mismatched DNA termini (predicted error frequency of ∼0.4; one error per three nucleotides synthesized), indicating that DNA polymerases enhance fidelity by a large factor.[51] DNA polymerase specificity is commonly characterized by determining the misinsertion frequency.[52] The misinsertion frequency is the insertion efficiency of an incorrect nucleotide divided by the sum of the insertion efficiencies for incorporation of incorrect and correct nucleotides at the same concentration of nucleotides. Quantitatively, fidelity is simply the reciprocal of the misinsertion frequency. In general, the specificity constants for incorrect nucleotides are much lower than for the correct nucleotide, so that fidelity is simply the ratio of specificity constants $[(k_{cat}/K_m)_{corr}/(k_{cat}/K_m)_{incorr}]$. Because relative misinsertion efficiency and fidelity are the simple ratio of specificity constants for insertion of correct and incorrect nucleotides, they can be altered by a change in one specificity constant or both.

Importantly, low- and high-fidelity polymerases insert incorrect nucleotides with similar efficiencies.[53] Consequently, fidelity is modulated by the efficiency of correct nucleotide insertion, and the molecular strategies that contribute to efficient DNA synthesis are dependent on the specific polymerase. Thus, an understanding of fidelity at the molecular level requires structural insight into the attributes that contribute to correct insertion efficiency rather than the molecular interactions that may occur between a low-fidelity polymerase during incorrect insertion. The lower efficiency and fidelity of DNA synthesis displayed by Y-family DNA polymerases is most likely reflected in the positioning of charged active site residues in the catalytic core.[23] As noted previously,[45] X- and Y-family DNA polymerases do not exhibit a conserved basic side chain interacting with a nonbridging oxygen of the α-phosphate. The lack of this interaction would be expected to diminish the rate of correct nucleotide insertion, thereby decreasing fidelity.

Induced Fit. The induced-fit hypothesis proposes that ligand-induced conformational changes align catalytic groups for optimal activity.[54] Poor substrates would deter catalysis through the misalignment of the reactive atoms. As described above, crystallographic structures of polymerase binary DNA and ternary (+dNTP) complexes indicate that the N-subdomain closes around the nascent base pair.[55] For 25 years, researchers characterizing the polymerase reaction have attempted to show that correct nucleotide insertion was limited by a nonchemical step. For most DNA polymerases, small elemental effects on the rate of nucleotide insertion of α-thio-substituted nucleotide analogues relative to the natural substrates were provided as evidence that chemistry was only partially rate-limiting. On the basis of model compounds, a significant decrease in rate upon sulfur substitution would suggest that chemistry is rate-limiting. However, there appears to be significant steric considerations, in addition to the electronegativity of sulfur, that influence the measured rate.[56] Following polymerase−DNA conformational changes with fluorescently labeled DNA and the effect of viscosity on both nucleotide insertion and fluorescent transients, the Tsai laboratory has provided compelling evidence that for pol β, chemistry is generally rate-limiting for nucleotide insertion.[57−59] Likewise, Sucato et al.[60,61] and Oertell et al.[62] employing nucleotide analogues that alter the pK_a of the leaving group provide direct kinetic evidence that the rate-determining step during transient-state nucleotide insertion involves bond breaking in the transition state.

A significant effort has been invested in determining the identity of the rate-determining step because it was assumed that a rate-limiting conformational change must limit correct nucleotide insertion for polymerases that utilize an induced-fit model. However, Post and Ray[63] have pointed out that induced fit can alter enzyme specificity even when critical conformational changes are kinetically silent (i.e., fast), such as when the transition states for correct and incorrect nucleotide incorporation are unique. Additionally, they show that an induced-fit model reduces specificity. This reduced level of discrimination represents an acceptable compromise for an enzyme such as a DNA polymerase that must select a different and/or new substrate (DNA and dNTP) with each catalytic cycle.

More recently, Tsai and Johnson highlighted that catalytic efficiency (k_{cat}/K_m) of correct nucleotide insertion is independent of the chemical step (k_4) even when it is the slowest step in the forward direction.[14,64] Critically, efficiency is linked to the reversal of the polymerase conformational change (k_{-3}). Thus, the concentration of complex IV may accumulate

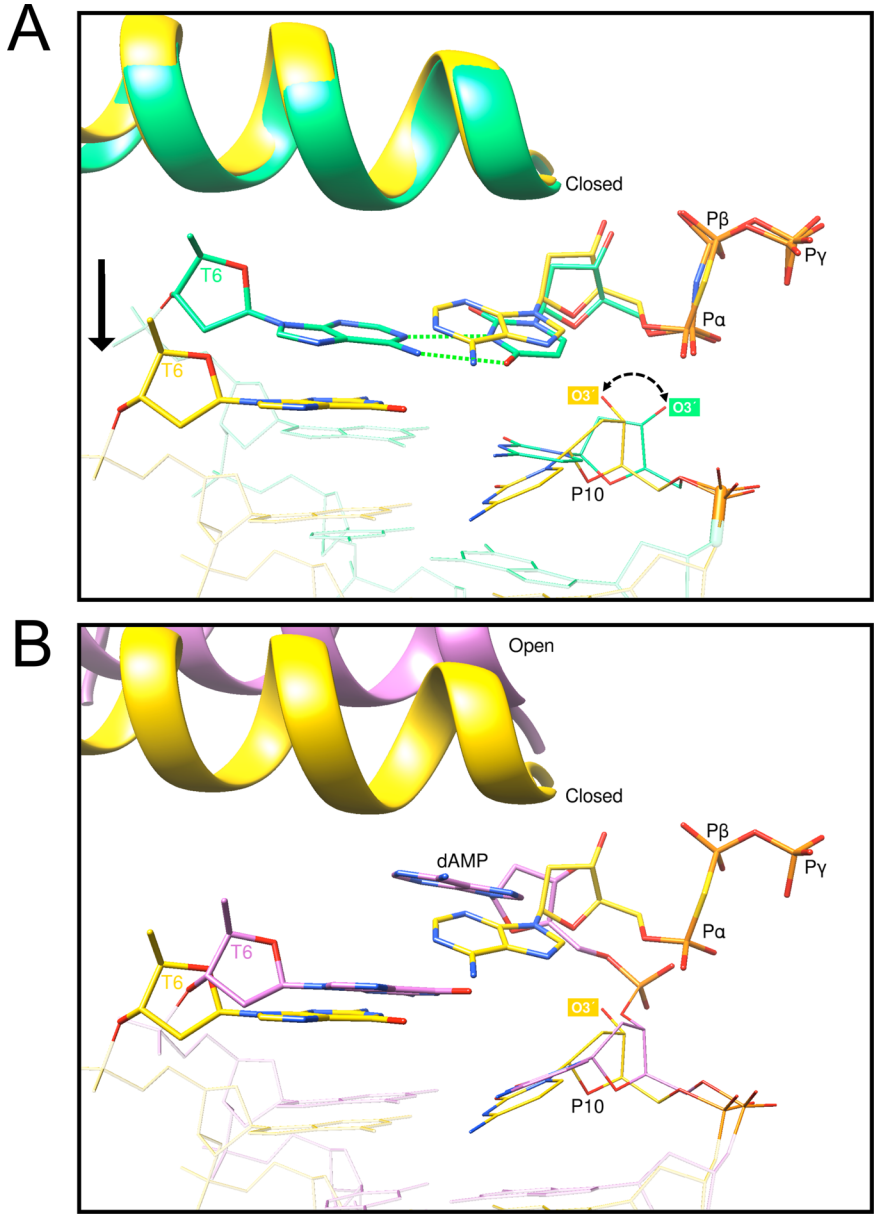

Figure 7. Intermediate pol β structures for insertion of the wrong nucleotide. (A) Overlay of the ternary substrate complex structure with a correct incoming nucleotide (PDB entry 2FMS, light green carbons) with a precatalytic complex with an active site mismatch (PDB entry 3C2M, yellow carbons; dG-dAMPCPP).[37,65] The position of α-helix N (ribbon) of the N-subdomain indicates that the polymerase is in the closed conformation. The coding template base (T6) is shifted upstream 3.2 Å, while the incoming nucleotide is positioned in the dNTP binding pocket. The α-, β-, and γ-phosphates of the incoming nucleotide are denoted Pα, Pβ, and Pγ, respectively. The primer terminus (P10) of the mismatched structure rotates to follow its templating base that has shifted upstream, as the coding templating nucleotide vacates its binding site. This displaces O3′ from the primer terminus (highlighted), thereby deterring incorrect nucleotide insertion. (B) In contrast to insertion of the correct nucleotide in the crystal, misinsertion of an incorrect nucleotide results in an open binary complex in which PP_i has dissociated (PDB entry 4KLU).[39] The structure of the binary product complex following misinsertion indicates that the enzyme is in the open conformation (pink carbons). In this open conformation, the density for the misinserted nucleotide is poor, indicating that it can assume multiple conformations.

for correct insertion, but not for incorrect insertion (i.e., the concentration of complex III is high because $k_{-3,\text{incorrect}} \gg k_{-3,\text{correct}}$). Consequently, the conformational change insulates the correct nucleotide from dissociating from the ternary substrate complex and commits it to the forward insertion reaction.

Structural Characterization of a Base Substitution Error. Crystallographic structures of pol β with an incoming incorrect nucleotide indicate that the ternary complex is in a closed conformation (Figure 7A).[39,65] Using a mutant enzyme that destabilizes the closed form suggests that the incorrect incoming nucleotide absolutely requires an active site nucleotide metal (sometimes termed metal B) for binding because the Watson−Crick edge of the base does not participate in initial binding, in contrast to that of a correct nucleotide (Figure 5A).[34] To accommodate the wrong incoming nucleotide in the closed polymerase conformation, the templating base vacates the coding position with an upstream shift in the template strand. The resulting pseudoabasic template site relieves potential steric conflicts with the wrong incoming nucleotide. Although hydrogen bonding is precluded, the kinetics of dATP insertion is similar

dx.doi.org/10.1021/bi500139h | *Biochemistry* 2014, 53, 2768−2780

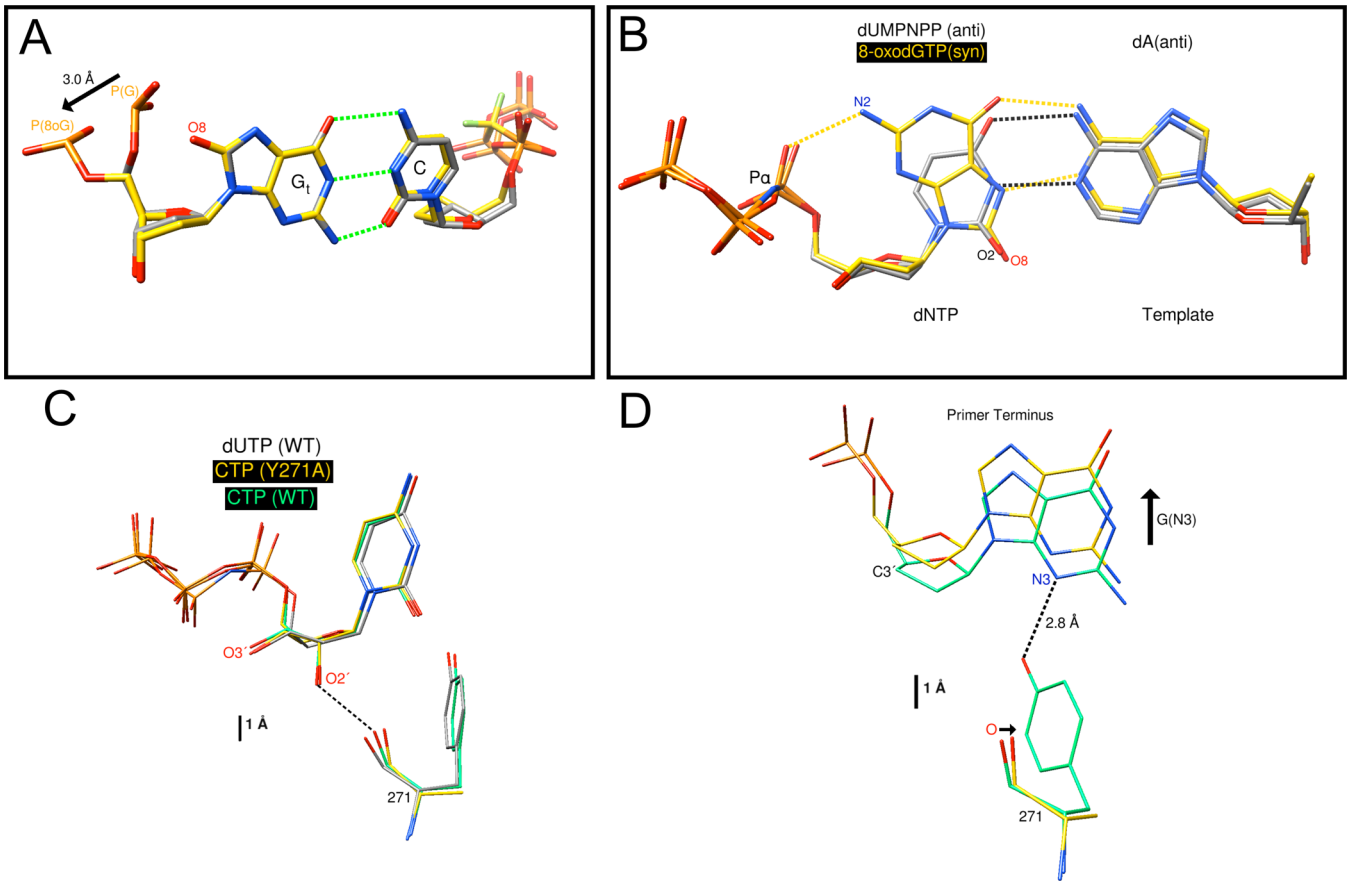

Figure 8. Structures of pol β with nonstandard substrates. (A) Structure of a ternary substrate complex with 8-oxoG in the templating position (G_t) paired with cytosine (PDB entry 3RJI, yellow carbons).[70] It is superimposed with a ternary substrate complex with a templating guanine (PDB entry 2FMP, gray carbons).[37] The bases are in an *anti* conformation, but the phosphate of the adducted guanine is repositioned to relieve steric and electrostatic clashes. (B) Structure of a ternary substrate complex with an incoming 8-oxodGTP in the *syn* conformation paired with adenine (PDB entry 3MBY, yellow carbons).[77] In contrast to a staggered arrangement of bases described previously with active site mismatches, the 8-oxodGTP-dA mispair is planar because 8-oxodGTP assumes the *syn* conformation while the templating deoxyadenine (dA) remains in the *anti* conformation providing for good Watson−Crick geometry. The *syn* conformation is stabilized through Hoogsteen hydrogen bonding with the templating adenine (yellow dashed lines) and a hydrogen bond with Asn279 (not shown). The *syn* conformation of 8-oxodGTP positions O8 in the DNA minor groove in a position similar to that of O2 for a Watson−Crick base pair. The structure of the ternary substrate complex with dUMPNPP paired with adenine is shown for reference (PDB entry 2FMS, gray carbons).[37] Additionally, an intramolecular hydrogen bond between N2 and a nonbridging oxygen on Pα (pro-S_P) of 8-oxodGTP could stabilize the *syn* conformer. (C) Structures of precatalytic ternary substrate complexes of pol β with an incoming CTP (wild-type enzyme, PDB entry 3RH4, light green carbons; Y271A mutant, PDB entry 3RH6, yellow carbons) were superimposed with the wild-type enzyme with an incoming dUMPNPP (PDB entry 2FMS, gray carbons).[37,73] The 2′-ribose oxygen is unusually close to the carbonyl oxygen of Tyr271 (2.54 Å, dashed line) but is well-accommodated in the closed complex of these structures. Replacing the tyrosine side chain with a methyl group (Y271A) provides additional freedom to subtly displace this carbonyl from O2′, resulting in a mutant enzyme that displays a decreased level of discrimination for ribonucleotides.[73] (D) Tyr271 hydrogen bonds to the base of the minor groove edge of the primer terminus (dashed black line). Substitution of Tyr271 with alanine results in the loss of this hydrogen bond and displacement of the dideoxy-terminated primer into the major groove. This is illustrated by examining the position of N3 of the guanine base in the structures of wild-type and mutant enzymes with an incoming CTP. The carbonyl of Ala271 is also illustrated.

to that observed for a true abasic site.[66] Importantly, the shift in the template strand results in rotation of the primer terminus as it remains hydrogen bonded to its templating base. The rotation of the primer terminus displaces O3′ to a position that deters misinsertion (Figure 7B). Misinsertion would require that the primer terminus sugar realign through transient template strand slippage (i.e., partially subdomain opening) or melting of the primer terminus from the template strand.

In contrast to the stable closed conformation observed after correct insertion, crystallographic structures after nucleotide misinsertion demonstrate that the N-subdomain can open and release PP_i and metals.[39] The phosphate of the misinserted nucleotide has rotated to a position that would deter further DNA synthesis (i.e., stalling primer elongation). As a result, a product-associated metal is not observed because this phosphate group contributes important stabilizing ligands with the product metal. The only stable conformation for the misinserted adenine is where it stacks over the templating guanine, but the sugar and base exhibit poor electron density, indicating that the nascent terminus is dynamic.[39]

Oxidative DNA Damage. Environmental and endogenous toxic chemicals lead to oxidative stress that threatens the integrity of genomic DNA. Cells maintain an intricate surveillance system for protecting themselves against adverse genotoxic stress. A major lesion found in DNA and dNTP pools exposed to reactive oxygen species is the promutagenic lesion 8-oxo-7,8-dihydro-2′-deoxyguanosine (8-oxoG). Thus, oxidative stress leads to production of 8-oxodGTP in the dNTP

dx.doi.org/10.1021/bi500139h | *Biochemistry* 2014, 53, 2768−2780

pool and 8-oxoG in DNA. At neutral pH, the major tautomeric form of 8-oxoG has a carbonyl group at C8 and is protonated at N7. Thus, guanine oxidation results in the alteration of the hydrogen bonding capacity of its Hoogsteen edge. Whereas the unmodified deoxyguanine glycosidic torsion-angle preference is *anti*, 8-oxoG favors a *syn* conformation that can form a Hoogsteen base pair with adenine. The altered glycosidic torsion-angle preference is due to steric repulsion between O8 and deoxyribose. Although the 8-oxoG(*syn*)-A(*anti*) base pair does not exhibit Watson−Crick hydrogen bonding, this mispair is well-accommodated within duplex DNA.[67]

The mutagenic effects of 8-oxoG are mediated by the action of DNA polymerases, because the molecular interactions of 8-oxoG in the confines of the active site can influence its *anti*−*syn* conformation. Structural characterization of pol β ternary complex structures with DNA containing 8-oxoG indicates that the glycosidic torsion-angle preference is determined by its base pairing partner, being *anti* with a complementary cytosine and *syn* when base-paired with adenine.[68−70] The structures reveal that the template binding pocket will permit 8-oxoG to assume an *anti* or *syn* conformation and encode incorporation of an incoming cytosine or adenine, respectively. However, the binding pocket for the incoming nucleotide does not have this flexibility, so that insertion of 8-oxodGTP opposite cytosine is strongly discouraged.[70]

A binary complex crystal structure was obtained with 8-oxoG in the template position of the single-nucleotide gapped DNA substrate.[68,70] As expected, the enzyme is in the open conformation. In this binary complex structure with unpaired 8-oxoG, the 8-oxoG base could be modeled into the electron density in both the *syn* conformation and the *anti* conformation, indicating that the 8-oxoG is in conformational equilibrium in the absence of enzyme; once the enzyme is bound, the base is sterically restrained from altering its general glycosidic angle. In this case, the 8-oxoG base may be available for pairing with an incoming dATP or dCTP. Similarly, the structure of the phosphate backbone of the 5′-phosphate of the 8-oxoG nucleotide suggests two positions similar to that observed with alternate templating bases [G and 8-oxoG (see below)].

Structures of preinsertion complexes of 8-oxoG paired with an incoming dCTP or ddCTP in the confines of the pol β active site have been determined.[68−70] The N-subdomain is in the closed conformation with the bases of the nascent base pair in *anti* conformations. Only a minor change in the phosphate backbone conformation of the templating 8-oxoG is required to relieve the steric clash of O8 with the sugar−phosphate backbone (Figure 8A). A ternary complex structure of pol β with 8-oxoG as the templating base and an incoming nonhydrolyzable nucleotide analogue, dAMPCPP, has also been determined.[70] In this case, the templating base 8-oxoG is in a *syn* conformation and forms a Hoogsteen base pair with the incoming adenine. The *syn* conformation of 8-oxoG is stabilized by stacking with an adjacent lysine residue (Lys280).

In contrast to the template binding pocket, there is a severe constraint for the incoming nucleotide for insertion of 8-oxodGTP.[70] This is expressed kinetically as moderate insertion efficiency for 8-oxodGTP opposite adenine and a severely reduced efficiency opposite cytosine. The structure of a ternary complex of 8-oxodGTP opposite adenine indicates that 8-oxodGTP assumes the *syn* conformation and forms a Hoogsteen base pair with the templating adenine (Figure 8B). In contrast to previously published structures of pol β with active site mismatches, this mispair is planar and exhibits Watson−Crick-like geometry, albeit with Hoogsteen hydrogen bonds. The *syn* conformation of 8-oxodGTP is stabilized through Hoogsteen hydrogen bonding with the templating adenine, a hydrogen bond with Asn279, and an intramolecular hydrogen bond between N2 and a nonbridging oxygen on the α-phosphate.

For most DNA polymerases, 8-oxodGTP is preferentially misinserted opposite adenine rather than cytosine.[70] This is consistent with the lack of polymerase crystal structures with 8-oxodGTP paired with a templating cytosine. Modeling an incoming 8-oxodGTP in an *anti* conformation paired with cytosine indicates that steric repulsion between O8 and its deoxyribose phosphate would distort the active site. Although DNA polymerases can modulate the backbone position of the templating nucleotide, perturbing the position of the α-phosphate of the incoming 8-oxodGTP to accommodate an *anti* conformation would be expected to severely compromise its insertion.

Recent progress in understanding the structural basis of 8-oxoG mutagenesis by DNA polymerases has provided insight into how the architecture of the DNA polymerase active site is able to adapt to the Hoogsteen base pair. All DNA polymerases can accommodate a Hoogsteen base pair with an 8-oxoG(*syn*)-A(*anti*) mispair much more effectively than with a G-A mispair. Ultimately, discrimination will rely on the effect of the *anti*−*syn* equilibrium imposed on 8-oxoG by the DNA polymerase active site.

Sugar Discrimination. Ribonucleoside triphosphates differ from their deoxynucleotide counterparts by a single atom (oxygen) at C2′ of the sugar, and their cellular concentrations significantly exceed those of dNTPs. Thus, ribonucleotides would be inserted during DNA replication and repair at frequencies much higher than those observed for deoxynucleotides with the wrong base. The presence of a ribose 2′-hydroxyl group stabilizes the glycosyl bond but makes the DNA phosphodiester backbone more susceptible to hydrolysis. Spontaneous or enzyme-catalyzed DNA strand breaks initiate repair and cellular signaling events that would impact overall genome stability and cell survival.

In most instances, DNA polymerases discriminate against ribonucleotide insertion by binding them weakly and inserting them more slowly than their natural substrate.[71] Crystallographic structures of substrate complexes of DNA polymerases from different families have indicated that a side chain could sterically interfere with binding of a ribonucleoside triphosphate. This side chain has been termed a "steric gate".[72] In contrast, X-family DNA polymerases deter insertion of ribonucleotides using the protein backbone near the carboxyl terminus of α-helix M [i.e., Tyr271 of pol β (Figure 8C)].[73] The backbone carbonyl of Tyr271 would be expected to clash with the hydroxyl group on C2′ of the incoming ribonucleotide. This would be expected to have important consequences because after binding a deoxynucleotide, α-helix M rotates so that Tyr271 forms a hydrogen bond with the minor groove edge of the primer terminus (Figure 8D). Therefore, ribonucleotide binding could alter interactions at the primer terminus transmitted through the altered interactions with α-helix M.

Wild-type pol β inserts ribonucleotides with an efficiency comparable to those of other polymerases that have been examined.[71] With a decrease in the size of the side chain of residue 271 by alanine substitution (i.e., Y271A), the level of

pol β ribonucleotide discrimination decreases.[73] Surprisingly, ternary substrate complex structures of wild-type and Y271A pol β with an incoming CTP indicated that the incoming ribonucleotide is well-accommodated in the nascent base pair binding pocket of pol β (Figure 8C). Comparing the crystallographic structures of the wild-type enzyme with bound dCTP or CTP and that of the Y271A mutant with CTP reveals that Tyr271 appears to play two significant roles in ribonucleotide discrimination. The backbone carbonyl at Tyr271 gets unfavorably close to 2′-OH of the ribose in the wild-type structure, and the structure of the mutant indicates that this carbonyl attempts to move farther from O2′ of the incoming ribonucleotide (Figure 8C). Quantum calculations suggest that the energetic cost for the proximity between the backbone carbonyl and ribose O2′ was only ∼2.2 kcal/mol, similar to the observed loss of binding affinity when the wild-type enzyme binds ribonucleotides.[73] Thus, favorable interactions in one region of an enzyme can overcome smaller repulsive interactions in adjacent regions. Significantly, the alanine side chain also removes a hydrogen bond between the tyrosine hydroxyl group and the minor groove edge of the primer terminal base in the closed ternary substrate conformation (Figure 8D). In the wild-type enzyme, this hydrogen bond may alter the active site geometry, thereby deterring insertion of substrates with the wrong sugar. Therefore, discrimination of the ribonucleotide by pol β is attributed to the loss of a contact with the primer terminus and a steric clash between O2′ of the ribose ring and the adjacent polymerase backbone carbonyl.

The dNTP binding affinity for many DNA polymerases is in the range of concentrations found in cells. Although DNA polymerases bind ribonucleotides weakly, their elevated concentration in the cell would permit them to effectively compete for binding. Although ribonucleotides may not be incorporated, they would impact the rate of DNA polymerization. In contrast, because RNA polymerases bind dNTPs weakly and their cellular concentration is low, dNTPs would exert a weaker impact on RNA polymerization.

FUTURE OUTLOOK

Structural, kinetic, and computational approaches have provided powerful tools for the development of molecular insights into DNA polymerase function. These experimental approaches indicate that dynamic events within the protein, substrates, and cofactors underlie molecular events that hasten correct and deter incorrect DNA synthesis. The observation that additional divalent metals may participate in catalysis, in addition to the two metals that have been traditionally proposed, provides additional motivation to probe chemistry in greater detail. Clearly, the highly charged active site provides an environment that could modulate chemistry through subtle molecular (charge and position) changes. Although the experimental focus has been on the forward DNA synthesis reaction, further characterization of the reverse reaction, pyrophosphorolysis, is warranted, especially because the reverse reaction can play an important role in nucleoside drug resistance.[74,75] Additionally, solution studies indicate that divalent metals can influence the conformational equilibrium (open−closed) of the pol β DNA binary complex that would influence the distribution of active enzyme species.[40]

DNA polymerases often have accessory factors, and our understanding of the kinetic and structural effects these factors have on substrate binding and chemistry is lacking. Likewise, how substrates and/or products are optimally processed through a pathway with several enzymes (substrate channeling) provides important experimental opportunities that will certainly uncover cellular strategies for enhancing enzyme efficiency. The polymerase's ability to replicate DNA of varying sequence with high fidelity represents an evolutionary achievement that perpetuates life and evolution. The elegant mechanisms that contribute to this elementary reaction are finally being uncovered. Even though structural biology has uncovered key molecular details during DNA synthesis, there are sure to be new details that have not been considered.

AUTHOR INFORMATION

Corresponding Author

*E-mail: wilson5@niehs.nih.gov. Phone: (919) 541-3267.

Funding

This research was supported by Research Projects Z01-ES050158 and Z01-ES050159 (S.H.W.) of the Intramural Research Program of the National Institute of Environmental Health Sciences and was in association with National Institutes of Health Grant 1U19CA105010.

Notes

The authors declare no competing financial interest.

ACKNOWLEDGMENTS

We recognize the significant contributions of Drs. J. M. Krahn, V. K. Batra, and B. D. Freudenthal for their structural characterizations. Structural images were produced using the Chimera package[76] from the Resource for Biocomputing, Visualization, and Informatics at the University of California, San Francisco (supported by National Institutes of Health Grant P41 RR-01081).

ABBREVIATIONS

8-oxoG, 8-oxo-7,8-dihydro-2′-deoxyguanosine; AP, apurinic/apyrimidinic; BER, base excision repair; C-subdomain, catalytic subdomain; D-subdomain, DNA binding subdomain; dNTP, deoxynucleoside triphosphate; dRP, deoxyribose phosphate; HhH, helix−hairpin−helix; N-subdomain, nascent base pair binding subdomain; PDB, Protein Data Bank; pol, DNA polymerase; PP_i, pyrophosphate.

REFERENCES

(1) Braithwaite, D. K., and Ito, J. (1993) Compilation, alignment, and phylogenetic relationships of DNA polymerases. *Nucleic Acids Res. 21*, 787−802.

(2) Beard, W. A., and Wilson, S. H. (2000) Structural design of a eukaryotic DNA repair polymerase: DNA polymerase β. *Mutat. Res. 460*, 231−244.

(3) Beard, W. A., and Wilson, S. H. (2006) Structure and mechanism of DNA polymerase β. *Chem. Rev. 106*, 361−382.

(4) Nakamura, J., and Swenberg, J. A. (1999) Endogenous apurinic/apyrimidinic sites in genomic DNA of mammalian tissues. *Cancer Res. 59*, 2522−2526.

(5) Lindahl, T., and Nyberg, B. (1972) Rate of depurination of native deoxyribonucleic acid. *Biochemistry 11*, 3610−3618.

(6) Moon, A. F., Garcia-Diaz, M., Batra, V. K., Beard, W. A., Bebenek, K., Kunkel, T. A., Wilson, S. H., and Pedersen, L. C. (2007) The X family portrait: Structural insights into biological functions of X family polymerases. *DNA Repair 6*, 1709−1725.

(7) Bebenek, K., Pedersen, L. C., and Kunkel, T. A. (2014) Structure−function studies of DNA polymerase λ. *Biochemistry 53*, DOI: 10.1021/bi4017236.

(8) Sobol, R. W., Horton, J. K., Kühn, R., Gu, H., Singhal, R. K., Prasad, R., Rajewsky, K., and Wilson, S. H. (1996) Requirement of mammalian DNA polymerase β in base excision repair. *Nature 379*, 183−186.
(9) Horton, J. K., Joyce-Gray, D. F., Pachkowski, B. F., Swenberg, J. A., and Wilson, S. H. (2003) Hypersensitivity of DNA polymerase β null mouse fibroblasts reflects accumulation of cytotoxic repair intermediates from site-specific alkyl DNA lesions. *DNA Repair 2*, 27−48.
(10) Prasad, R., Williams, J. G., Hou, E. W., and Wilson, S. H. (2012) Pol β associated complex and base excision repair factors in mouse fibroblasts. *Nucleic Acids Res. 40*, 11571−11582.
(11) Wallace, S. S., Murphy, D. L., and Sweasy, J. B. (2012) Base excision repair and cancer. *Cancer Lett. 327*, 73−89.
(12) Sweasy, J. B., Lang, T., and DiMaio, D. (2006) Is base excision repair a tumor suppressor mechanism? *Cell Cycle 5*, 250−259.
(13) Nemec, A. A., Donigan, K. A., Murphy, D. L., Jaeger, J., and Sweasy, J. B. (2012) Colon cancer-associated DNA polymerase β variant induces genomic instability and cellular transformation. *J. Biol. Chem. 287*, 23840−23849.
(14) Johnson, K. A. (2008) Role of induced fit in enzyme specificity: A molecular forward/reverse switch. *J. Biol. Chem. 283*, 26297−26301.
(15) Tanabe, K., Bohn, E. W., and Wilson, S. H. (1979) Steady-state kinetics of mouse DNA polymerase β. *Biochemistry 18*, 3401−3406.
(16) Schlick, T., Arora, K., Beard, W. A., and Wilson, S. H. (2012) Perspective: Pre-chemistry conformational changes in DNA polymerase mechanisms. *Theor. Chem. Acc. 131*, 1287.
(17) Beard, W. A., and Wilson, S. H. (1995) Purification and domain-mapping of mammalian DNA polymerase β. *Methods Enzymol. 262*, 98−107.
(18) Sawaya, M. R., Pelletier, H., Kumar, A., Wilson, S. H., and Kraut, J. (1994) Crystal structure of rat DNA polymerase β: Evidence for a common polymerase mechanism. *Science 264*, 1930−1935.
(19) Kim, S. J., Lewis, M. S., Knutson, J. R., Porter, D. K., Kumar, A., and Wilson, S. H. (1994) Characterization of the tryptophan fluorescence and hydrodynamic properties of rat DNA polymerase β. *J. Mol. Biol. 244*, 224−235.
(20) Tang, K.-H., Niebuhr, M., Aulabaugh, A., and Tsai, M.-D. (2008) Solution structures of 2:1 and 1:1 DNA polymerase-DNA complexes probed by ultracentrifugation and small-angle X-ray scattering. *Nucleic Acids Res. 36*, 849−860.
(21) Matsumoto, Y., and Kim, K. (1995) Excision of deoxyribose phosphate residues by DNA polymerase β during DNA repair. *Science 269*, 699−702.
(22) Piersen, C. E., Prasad, R., Wilson, S. H., and Lloyd, R. S. (1996) Evidence for an imino intermediate in the DNA polymerase β deoxyribose phosphate excision reaction. *J. Biol. Chem. 271*, 17811−17815.
(23) Wu, S., Beard, W. A., Pedersen, L. G., and Wilson, S. H. (2014) Structural comparison of DNA polymerase architecture suggests a nucleotide gateway to the polymerase active site. *Chem. Rev. 114*, 2759−2774.
(24) Ollis, D. L., Brick, P., Hamlin, R., Xuong, N. G., and Steitz, T. A. (1985) Structure of large fragment of *Escherichia coli* DNA polymerase I complexed with dTMP. *Nature 313*, 762−766.
(25) Xia, S., and Konigsberg, W. H. (2014) RB69 DNA polymerase: Structure, kinetics, and fidelity. *Biochemistry 53*, DOI:10.1021/bi4014215.
(26) Yang, W. (2014) A summary of Y-family DNA polymerases and a case study of human polymerase η. *Biochemistry 53*, DOI: 10.1021/bi500019s.
(27) Beard, W. A., Shock, D. D., Yang, X.-P., DeLauder, S. F., and Wilson, S. H. (2002) Loss of DNA polymerase β stacking interactions with templating purines, but not pyrimidines, alters catalytic efficiency and fidelity. *J. Biol. Chem. 277*, 8235−8242.
(28) Prasad, R., Beard, W. A., and Wilson, S. H. (1994) Studies of gapped DNA substrate binding by mammalian DNA polymerase β: Dependence on 5′-phosphate group. *J. Biol. Chem. 269*, 18096−18101.
(29) Prasad, R., Shock, D. D., Beard, W. A., and Wilson, S. H. (2010) Substrate channeling in mammalian base excision repair pathways: Passing the baton. *J. Biol. Chem. 285*, 40479−40488.
(30) Sawaya, M. R., Prasad, P., Wilson, S. H., Kraut, J., and Pelletier, H. (1997) Crystal structures of human DNA polymerase β complexed with gapped and nicked DNA: Evidence for an induced fit mechanism. *Biochemistry 36*, 11205−11215.
(31) Mullen, G. P., Antuch, W., Maciejewski, M. W., Prasad, R., and Wilson, S. H. (1997) Insights into the mechanism of the β-elimination catalyzed by the N-terminal domain of DNA polymerase β. *Tetrahedron 53*, 12057−12066.
(32) Deterding, L. J., Prasad, R., Mullen, G. P., Wilson, S. H., and Tomer, K. B. (2000) Mapping of the 5′-2-deoxyribose-5-phosphate lyase active site in DNA polymerase β by mass spectrometry. *J. Biol. Chem. 275*, 10463−10471.
(33) Beard, W. A., Shock, D. D., and Wilson, S. H. (2004) Influence of DNA structure on DNA polymerase β active site function: Extension of mutagenic DNA intermediates. *J. Biol. Chem. 279*, 31921−31929.
(34) Freudenthal, B. D., Beard, W. A., and Wilson, S. H. (2012) Structures of dNTP intermediate states during DNA polymerase active site sssembly. *Structure 20*, 1829−1837.
(35) Beard, W. A., Osheroff, W. P., Prasad, R., Sawaya, M. R., Jaju, M., Wood, T. G., Kraut, J., Kunkel, T. A., and Wilson, S. H. (1996) Enzyme-DNA interactions required for efficient nucleotide incorporation and discrimination in human DNA polymerase β. *J. Biol. Chem. 271*, 12141−12144.
(36) Pelletier, H., Sawaya, M. R., Kumar, A., Wilson, S. H., and Kraut, J. (1994) Structures of ternary complexes of rat DNA polymerase β, a DNA template-primer, and ddCTP. *Science 264*, 1891−1903.
(37) Batra, V. K., Beard, W. A., Shock, D. D., Krahn, J. M., Pedersen, L. C., and Wilson, S. H. (2006) Magnesium induced assembly of a complete DNA polymerase catalytic complex. *Structure 14*, 757−766.
(38) Upton, T. G., Kashemirov, B. A., McKenna, C. E., Goodman, M. F., Prakash, G. K. S., Kultyshev, R., Batra, V. K., Shock, D. D., Pedersen, L. C., Beard, W. A., and Wilson, S. H. (2009) α,β-Diflurormethylene deoxynucleoside 5′-triphosphates: A convenient synthesis of useful probes for DNA polymerase β structure and function. *Org. Lett. 11*, 1883−1886.
(39) Freudenthal, B. D., Beard, W. A., Shock, D. D., and Wilson, S. H. (2013) Observing a DNA polymerase choose right from wrong. *Cell 154*, 157−168.
(40) Kirby, T. W., DeRose, E. F., Cavanaugh, N. A., Beard, W. A., Shock, D. D., Mueller, G. A., Wilson, S. H., and London, R. E. (2012) Metal-induced DNA translocation leads to DNA polymerase conformational activation. *Nucleic Acids Res. 40*, 2974−2983.
(41) Lang, T., Dalal, S., Chikova, A., DiMaio, D., and Sweasy, J. B. (2007) The E295K DNA polymerase β gastric cancer-associated variant interferes with base excision repair and induces cellular transformation. *Mol. Cell. Biol. 27*, 5587−5596.
(42) Li, Y., Gridley, C. L., Jaeger, J., Sweasy, J. B., and Schlick, T. (2012) Unfavorable electrostatic and steric interactions in DNA polymerase β E295K mutant interfere with the enzyme's pathway. *J. Am. Chem. Soc. 134*, 9999−10010.
(43) Balbo, P. B., Wang, E. C.-W., and Tsai, M.-D. (2011) Kinetic mechanism of active site assembly and chemical catalysis of DNA polymerase β. *Biochemistry 50*, 9865−9875.
(44) Nakamura, T., Zhao, Y., Yamagata, Y., Hua, Y.-j., and Yang, W. (2012) Watching DNA polymerase η make a phosphodiester bond. *Nature 487*, 196−201.
(45) Beard, W. A., and Wilson, S. H. (2003) Structural insights into the origins of DNA polymerase fidelity. *Structure 11*, 489−496.
(46) Arndt, J. W., Gong, W., Zhong, X., Showalter, A. K., Liu, J., Dunlap, C. A., Lin, Z., Paxson, C., Tsai, M.-D., and Chan, M. K. (2001) Insight into the catalytic mechanism of DNA polymerase β: Structures of intermediate complexes. *Biochemistry 40*, 5368−5375.
(47) Patel, S. S., Wong, I., and Johnson, K. A. (1991) Pre-steady-state kinetic analysis of processive DNA replication including complete

characterization of an exonuclease-deficient mutant. *Biochemistry 30*, 511−525.
(48) Lin, P., Pedersen, L. C., Batra, V. K., Beard, W. A., Wilson, S. H., and Pedersen, L. G. (2006) Energy analysis of chemistry for correct insertion by DNA polymerase β. *Proc. Natl. Acad. Sci. U.S.A. 103*, 13294−13299.
(49) Batra, V. K., Perera, L., Lin, P., Shock, D. D., Beard, W. A., Pedersen, L. C., Pedersen, L. G., and Wilson, S. H. (2013) Amino acid substitution in the active site of DNA polymerase β explains the energy barrier of the nucleotidyl transfer reaction. *J. Am. Chem. Soc. 135*, 8078−8088.
(50) Kunkel, T. A., and Bebenek, K. (2000) DNA replication fidelity. *Annu. Rev. Biochem. 69*, 497−529.
(51) Petruska, J., Goodman, M. F., Boosalis, M. S., Sowers, L. C., Cheong, C., Tonoco, J., and Ignacio (1988) Comparison between DNA melting thermodynamics and DNA polymerase fidelity. *Proc. Natl. Acad. Sci. U.S.A. 85*, 6252−6256.
(52) Fersht, A. R., Knill-Jones, J. W., and Tsui, W. C. (1982) Kinetic basis of spontaneous mutation: Misinsertion frequencies, proofreading specificities and cost of proofreading by DNA polymerases of *Escherichia coli*. *J. Mol. Biol. 156*, 37−51.
(53) Beard, W. A., Shock, D. D., Vande Berg, B. J., and Wilson, S. H. (2002) Efficiency of correct nucleotide insertion governs DNA polymerase fidelity. *J. Biol. Chem. 277*, 47393−47398.
(54) Koshland, D. E., Jr. (1958) Application of a theory of enzyme specificity to protein synthesis. *Proc. Natl. Acad. Sci. U.S.A. 44*, 98−104.
(55) Doublié, S., Sawaya, M. R., and Ellenberger, T. (1999) An open and closed case for all polymerases. *Structure 7*, R31−R35.
(56) Joyce, C. M., and Benkovic, S. J. (2004) DNA polymerase fidelity: Kinetics, structure, and checkpoints. *Biochemistry 43*, 14317−14324.
(57) Bakhtina, M., Lee, S., Wang, Y., Dunlap, C., Lamarche, B., and Tsai, M.-D. (2005) Use of viscogens, dNTPαS, and rhodium(III) as probes in stopped-flow experiments to obtain new evidence for the mechanism of catalysis by DNA polymerase β. *Biochemistry 44*, 5177−5187.
(58) Bakhtina, M., Roettger, M. P., Kumar, S., and Tsai, M. D. (2007) A unified kinetic mechanism applicable to multiple DNA polymerases. *Biochemistry 46*, 5463−5472.
(59) Bakhtina, M., Roettger, M. P., and Tsai, M.-D. (2009) Contribution of the reverse rate of the conformational step to polymerase β fidelity. *Biochemistry 48*, 3197−3208.
(60) Sucato, C. A., Upton, T. G., Kashemirov, B. A., Batra, V. K., Martinek, V., Xiang, Y., Beard, W. A., Pedersen, L. C., Wilson, S. H., McKenna, C. E., Florian, J., Warshel, A., and Goodman, M. F. (2007) Modifying the β,γ leaving-group bridging oxygen alters nucleotide incorporation efficiency, fidelity, and the catalytic mechanism of DNA polymerase β. *Biochemistry 46*, 461−471.
(61) Sucato, C. A., Upton, T. G., Kashemirov, B. A., Osuna, J., Oertell, K., Beard, W. A., Wilson, S. H., Florian, J., Warshel, A., McKenna, C. E., and Goodman, M. F. (2008) DNA polymerase β fidelity: Halomethylene-modified leaving groups in pre-steady-state kinetic analysis reveal differences at the chemical transition state. *Biochemistry 47*, 870−879.
(62) Oertell, K., Chamberlain, B. T., Wu, Y., Ferri, E., Kashemirov, B. A., Beard, W. A., Wilson, S. H., McKenna, C. E., and Goodman, M. F. (2014) Transition state in DNA polymerase β aatalysis: Rate-limiting chemistry altered by base-pair configuration. *Biochemistry 53*, 1842−1848.
(63) Post, C. B., and Ray, W. J., Jr. (1995) Reexamination of induced fit as a determinant of substrate specificity in enzymatic reactions. *Biochemistry 34*, 15881−15885.
(64) Tsai, Y.-C., and Johnson, K. A. (2006) A new paradigm for DNA polymerase specificity. *Biochemistry 45*, 9675−9687.
(65) Batra, V. K., Beard, W. A., Shock, D. D., Pedersen, L. C., and Wilson, S. H. (2008) Structures of DNA polymerase β with active site mismatches suggest a transient abasic site intermediate during misincorporation. *Mol. Cell 30*, 315−324.
(66) Beard, W. A., Shock, D. D., Batra, V. K., Pedersen, L. C., and Wilson, S. H. (2009) DNA polymerase β substrate specificity: Side chain modulation of the "A-rule". *J. Biol. Chem. 284*, 31680−31689.
(67) McAuley-Hecht, K. E., Leonard, G. A., Gibson, N. J., Thomson, J. B., Watson, W. P., Hunter, W. N., and Brown, T. (1994) Crystal structure of a DNA duplex containing 8-hydroxydeoxyguanine-adenine base pairs. *Biochemistry 33*, 10266−10270.
(68) Freudenthal, B. D., Beard, W. A., and Wilson, S. H. (2013) DNA polymerase minor groove interactions modulate mutagenic bypass of a templating 8-oxoguanine lesion. *Nucleic Acids Res. 41*, 1848−1858.
(69) Krahn, J. M., Beard, W. A., Miller, H., Grollman, A. P., and Wilson, S. H. (2003) Structure of DNA polymerase β with the mutagenic DNA lesion 8-oxodeoxyguanine reveals structural insights into its coding potential. *Structure 11*, 121−127.
(70) Batra, V. K., Shock, D. D., Beard, W. A., McKenna, C. E., and Wilson, S. H. (2012) Binary complex crystal structure of DNA polymerase β reveals multiple conformations of the templating 8-oxoguanine lesion. *Proc. Natl. Acad. Sci. U.S.A. 109*, 113−118.
(71) Cavanaugh, N. A., Beard, W. A., and Wilson, S. H. (2010) DNA polymerase β ribonucleotide discrimination: Insertion, misinsertion, extension, and coding. *J. Biol. Chem. 285*, 24457−24465.
(72) Brown, J. A., and Suo, Z. (2011) Unlocking the sugar 'steric gate' of DNA polymerases. *Biochemistry 50*, 1135−1142.
(73) Cavanaugh, N. A., Beard, W. A., Batra, V. K., Perera, L., Pedersen, L. G., and Wilson, S. H. (2011) Molecular insights into DNA polymerase deterrents for ribonucleotide insertion. *J. Biol. Chem. 286*, 31650−31660.
(74) Hanes, J. W., and Johnson, K. A. (2007) A novel mechanism of selectivity against AZT by the human mitochondrial DNA polymerase. *Nucleic Acids Res. 35*, 6973−6983.
(75) Meyer, P. R., Matsuura, S. E., So, A. G., and Scott, W. A. (1998) Unblocking of chain-terminated primer by HIV-1 reverse transcriptase through a nucleotide-dependent mechanism. *Proc. Natl. Acad. Sci. U.S.A. 95*, 13471−13476.
(76) Pettersen, E. F., Goddard, T. D., Huang, C. C., Couch, G. S., Greenblatt, D. M., Meng, E. C., and Ferrin, T. E. (2004) UCSF Chimera: A visualization system for exploratory research and analysis. *J. Comput. Chem. 25*, 1605−1612.
(77) Batra, V. K., Beard, W. A., Hou, E. W., Pedersen, L. C., Prasad, R., and Wilson, S. H. (2010) Mutagenic conformation of 8-oxo-7,8-dihydro-2′-dGTP in the confines of a DNA polymerase active site. *Nat. Struct. Mol. Biol. 17*, 889−890.
(78) Gridley, C. L., Rangarajan, S., Firbank, S., Dalal, S., Sweasy, J. B., and Jaeger, J. (2013) Structural changes in the hydrophobic hinge region adversely affect the activity and fidelity of the I260Q mutator DNA polymerase β. *Biochemistry 52*, 4422−4432.
(79) Krahn, J. M., Beard, W. A., and Wilson, S. H. (2004) Structural insights into DNA polymerase deterrents for misincorportion support an induced-fit mechanism for fidelity. *Structure 12*, 1823−1832.